



Combining punctual and ordinal contour data for accurate floodplain topography mapping

Carole Delenne, Jean-Stéphane Bailly, Mathieu Darteville, Nelly Marcy,
Antoine Rousseau

► To cite this version:

Carole Delenne, Jean-Stéphane Bailly, Mathieu Darteville, Nelly Marcy, Antoine Rousseau. Combining punctual and ordinal contour data for accurate floodplain topography mapping. *Spatial Accuracy 2016*, Jean-Stéphane Bailly; Didier Josselin, Jul 2016, Montpellier, France. pp.350-357. hal-01349737

HAL Id: hal-01349737

<https://hal.science/hal-01349737>

Submitted on 28 Jul 2016

HAL is a multi-disciplinary open access archive for the deposit and dissemination of scientific research documents, whether they are published or not. The documents may come from teaching and research institutions in France or abroad, or from public or private research centers.

L'archive ouverte pluridisciplinaire **HAL**, est destinée au dépôt et à la diffusion de documents scientifiques de niveau recherche, publiés ou non, émanant des établissements d'enseignement et de recherche français ou étrangers, des laboratoires publics ou privés.



Distributed under a Creative Commons Attribution - NonCommercial - NoDerivatives 4.0 International License

Combining punctual and ordinal contour data for accurate floodplain topography mapping

Carole Delenne^{*1,3}, Jean-Stéphane Bailly², Mathieu Dartevelle³, Nelly Marcy¹, Antoine Rousseau³

¹Univ. Montpellier, HSM, France

²AgroParisTech, LISAH, France

³INRIA, Lemon, France

*Corresponding author: carole.delenne@umontpellier.fr

I INTRODUCTION

Hydrodynamic models in two dimensions require a precise knowledge of the domain topography. However, as far as the modelling of great rivers or lakes is concerned, few accurate topographic records are generally available to accurately model the floodplain topography. The usual way to acquire accurate topographic information for hydraulics over floodplain remains the ground surveys, that provide punctual values at a very high cost. Based on these points, usual interpolation schemes often yield a too coarse and inaccurate topographic map for a realistic hydrodynamic modelling. Remote sensing data such as Lidar or stereo-photogrammetry data on non vegetated areas, constitute a good alternative to obtain large scale information, but yield other issues of acquisition and data processing. In addition, topographic Lidar operating with near-infrared lasers are still not suitable for an exhaustive survey of floodplains where submerged areas remain.

Progress in remote sensing data repeatability and spatial resolution now allows the automatic monitoring of water surfaces delineation from areal or satellite images either in optical or radar domains (see *e.g.* an application to the Inner Niger Delta in Ogilvie et al. (2015)). As for the recently launched Sentinel sensors, these data are becoming widely available with increasing spatial and temporal resolutions, allowing in turn the spatio-temporal monitoring of flooded areas. Flood dynamics from remote sensing data are known to be informative on floodplain topography for long (see *e.g.* Schumann et al. (2007) or Hostache et al. (2010)). Indeed, the extracted flooded areas may be considered as iso-elevation contour lines, as the hypothesis can be made that all the points located on the water/soil limit have the same elevation. If contour line elevation remains unknown, rank between the detected contour lines as well as between every contour line and surrounding topographic data points are known. Assuming this information, the next challenge is thus to develop a spatial data fusion method of ordered contour lines data and usual elevation data points to better model the floodplain topography.

Mixing punctual ranked and continuous data in spatial estimation was already proposed in literature, mainly to deal with highly skewed field distribution (Yamamoto, 2000) or for very large spatial datasets (Cressie and Johannesson, 2008). These methods used the uniform score transform and back-transform based on the standardized rank estimation (Saito and Goovaerts, 2000) to prevent the right estimate distribution and limit the smoothing effect of kriging. Uncertainty assessment of resulting punctual kriging estimates was proposed thanks to the transformation process (Yamamoto, 2007). Other methods also exist to quantify the uncertainty of contour lines in random fields (Lindgren and Rychlik, 1995; Wamelink and Saborowski, 2001). But in these studies, the objective was to quantify the uncertainty in contour lines location and not to quantify the uncertainty of contour lines level for a known location. Consequently, these

different studies only partly touched the problem we face.

The objective of this paper is to propose a method to estimate the elevation of the ranked contour lines from data points. This method starts from block conditional simulations estimates filtered on rank statistics. After contour line elevation estimate, a usual kriging is performed to reconstruct a topographic map over the floodplain. Starting from a synoptic and theoretical example, the principles, advantages, properties and limitations of the proposed method are exposed. The spatial accuracies obtained in contour lines estimates and topographic map are thus compared to the usual block kriging estimates.

II MATERIAL AND METHODS

2.1 Case study generation

A reference exhaustive elevation field $Z(s)$ on a floodplain D was generated from a Gaussian spatial covariance model with range 20, sill 1 and no nugget effect. The resulting field is centered on $\mu = 10$ and respects distribution $N(\mu, \sigma)$ (see Figure 1-left): the blue colours represent lower floodplain elevations meanwhile the yellow and green stem for higher elevation areas. D is a $100 \text{ m} \times 100 \text{ m}$ area and the dataset was generated on gridded D with resolution $r = 1 \text{ m}$, r denoting both the remote sensing image spatial resolution and the desired end-user topographic map resolution.

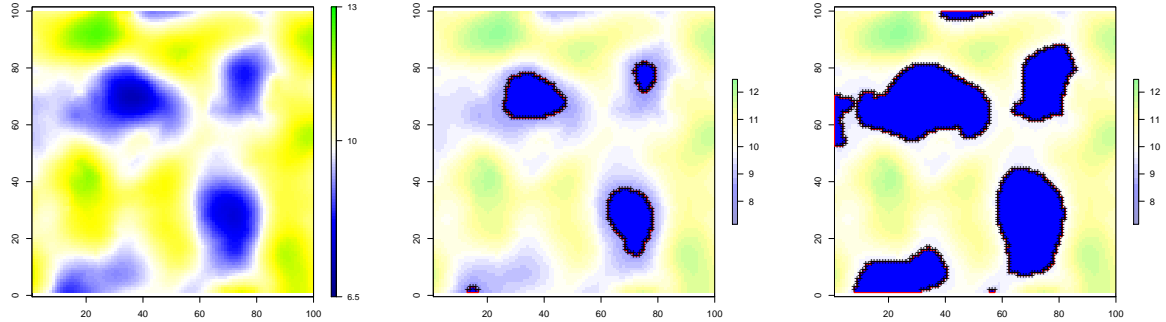


Figure 1: **Generated case study.** Left: Simulated elevation field over D ; Middle: flooded area at time 1 (blue) and resulting rasterized contour (black crosses); Right: flooded area at time 2 (blue) and resulting rasterized contour (black crosses).

To reproduce the remote sensing data support (Ogilvie et al., 2015), flooded areas were generated and delineated at resolution 0.5 m for two different times t_1 and t_2 during rising water: when areas lower than 9.5 m (Fig. 1-middle) and 8.5 m (Fig. 1-right) respectively are flooded. Contour polylines were generated from these rasterized flooded areas with 0.5 m spatial resolution. The sets of two generated contour polylines C_1 and C_2 were thus reduced to a set of polylines vertices s_i^j ($j \in (1, 2)$ denoting the polyline) regularly located along the lines (black cross on figures 1). C_1 and C_2 contained $n_1 = 201$ and $n_2 = 520$ points respectively. Four contour lines correspond to C_1 and five to C_2 (Fig. 1). When contour lines were connected to the D boundaries, only vertices within D were considered.

In addition, a sample of $n = 250$ topographic points $s_1 \dots s_n$ was randomly selected on D , excluding points selection at location closer than $b = 2 \text{ m}$ from polylines (Fig. 2-left). This ensures that no data points are located on a polyline, which would make too obvious the estimation

of its elevation. We further assume that contour polylines elevation is unknown but that ranks between the polylines (i.e. the polyline vertices s_i^j) and between polylines and surrounding topographic data points are known and may be computed (Fig. 2-right).

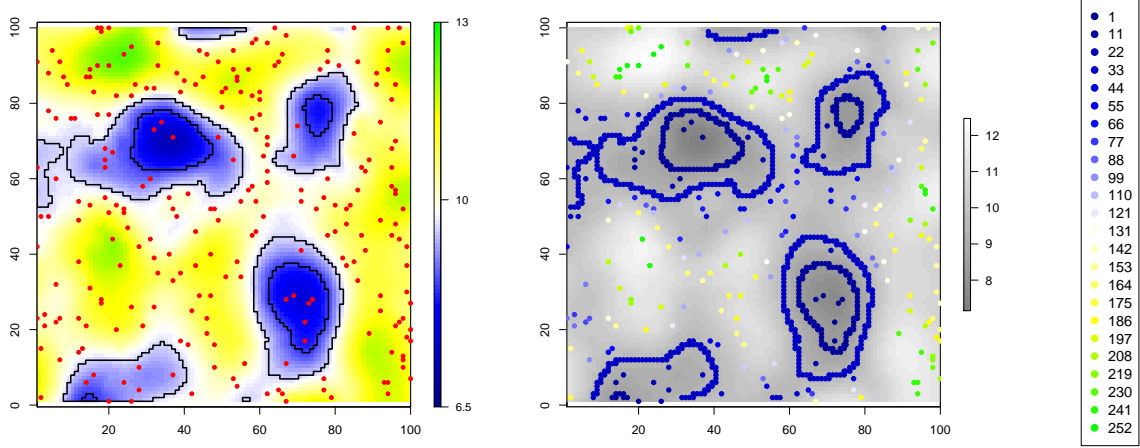


Figure 2: **Generated dataset.** Left: Simulated elevation field over D , contour polylines C_1 and C_2 (black lines) and data points (red points). Right: ranked data (points and polyline vertices) and according legend.

2.2 Method

The method we developed may be seen as a block conditional simulation process filtered by rank statistics, where a polyline C_j is seen as a block, *i.e.* a region corresponding to an unconnected set of vertices. Such simulation is known to be superior to kriging whenever interest lies in global statements for a region rather than inference on individual points. In the process described in the algorithm 1 hereafter, assuming a stationary random function, a spatial model (variogram) $\gamma(h)$ is first estimated and modelled from the 250 data points $s_1 \dots s_n$.

Algorithm 1 Contour polyline estimation process and field reconstruction

- 1: **for** $j = 1$ to $j = 2$ **do**
 - 2: Estimate and model the variogram $\gamma(h)$ from n data points
 - 3: Estimate ordinary kriging $\hat{z}_{ko}(s_i^j)$ on polyline vertices
 - 4: **for** $i = 1$ to $N = 100$ **do**
 - 5: Draw unconditional multigaussian simulation $z_{us}(s_k)$ and $z_{us}(s_i^j)$ on data location and polyline vertices
 - 6: Estimate ordinary kriging at vertices from simulated values at data locations $z_{ko}^*(s_i^j)$
 - 7: Compute conditional simulation on vertices (Eq. 1)
 - 8: Compute N polyline estimate by averaging vertices conditional simulations
 - 9: Filter keeping only polyline estimate conform to the initial ranks
 - 10: Compute polyline estimate \hat{z}_j averaging the kept polyline estimates
 - 11: Compute standard deviation estimate from the set of kept polyline estimates
 - 12: Affect polyline estimate \hat{z}_j to each polyline vertice s_i^j
 - 13: Perform ordinary kriging on all gridded D points from data $z(s_1) \dots z(s_n)$ and polyline vertices estimates $\hat{z}_j(s_i^j)$
-

Once the variogram $\gamma(h)$ is modelled, an ordinary kriging is performed on each polyline vertex. From the kriging, a first estimate of polyline elevation results from vertices averaging. For polyline C_j , we denote further \hat{z}_{ko}^j this estimate (corresponding to the usual block kriging estimate).

Next, a set of $N = 100$ conditional Multi-Gaussian simulations using the fitted variogram model and pathing through the 250 $s_1 \dots s_n$ is performed on each on the s_i^j contour vertices (Eq. 1):

$$z_{cs}(s_i^j) = \hat{z}_{ko}(s_i^j) + (z_{us}(s_i^j) - \hat{z}_{ko}^*(s_i^j)) \quad (1)$$

At the end of the conditional simulation, an estimate at polyline scale is computed by averaging simulated values on vertices. This remains consistent with the usual block kriging estimate since vertices are regularly located along the polyline.

$$\hat{z}_k^j = \frac{1}{n_j} \sum_{i=1}^{n_j} z_{cs}(s_i^j) \quad (2)$$

We thus obtain N elevation estimates $\hat{z}_k^j, k \in (1 \dots N)$ for a given contour polyline C_j . Only the estimates respecting the rank are kept in the following, yielding a set of M estimates ($M \leq N$) for a given polyline. From this set, the final estimate of polyline C_j becomes:

$$\hat{z}_j = \frac{1}{M} \sum_{k=1}^M \hat{z}_k^j \quad (3)$$

with uncertainty characterized by the standard deviation σ_{C_j} of the \hat{z}_k^j estimates.

In a final step, polyline estimate \hat{z}_j is affected to each polyline vertex s_i^j in order to perform, in addition to the 250 data points a gridded map using ordinary kriging.

III RESULTS

Results obtained for this theoretical test case are given in Figures 3 and 4. Figure 3-left shows the estimated empirical variogram (dots) and fitted variogram model (lines). Figure 3-right shows for C_1 and C_2 the resulting distribution of the estimates using conditional simulation, the final estimation equal to the average of conditional simulation (black vertical line) compared to the true value (blue vertical line) or the ordinary kriging (interpolation) estimate (red vertical line). In this first application, rank was always respected in the conditional simulation and for the ordinary kriging but, as shown in the following, this will not always be the case. The estimated elevation obtained for C_1 is 8.53 m (8.45 using ordinary kriging) for a true value equals to 8.5 m, with a standard deviation of the estimate being only 5.37e-03 m. For C_2 , the difference between the true elevation (9.5 m) and the estimated value is lower than one centimetre (3 cm using kriging) with standard deviation of the estimate equals to 3.99e-03 m.

Figure 4 shows the reconstructed fields from the method we proposed compared to *i*) the true field and *ii*) the field reconstructed only from the 250 data points without considering the contour polylines data. A visual comparison suggests better results for the proposed approach. However, artefacts can be seen around the pool located at the bottom-right corner of the domain. In this area, the elevation increases with the distance to the pool minimum but decreases again at

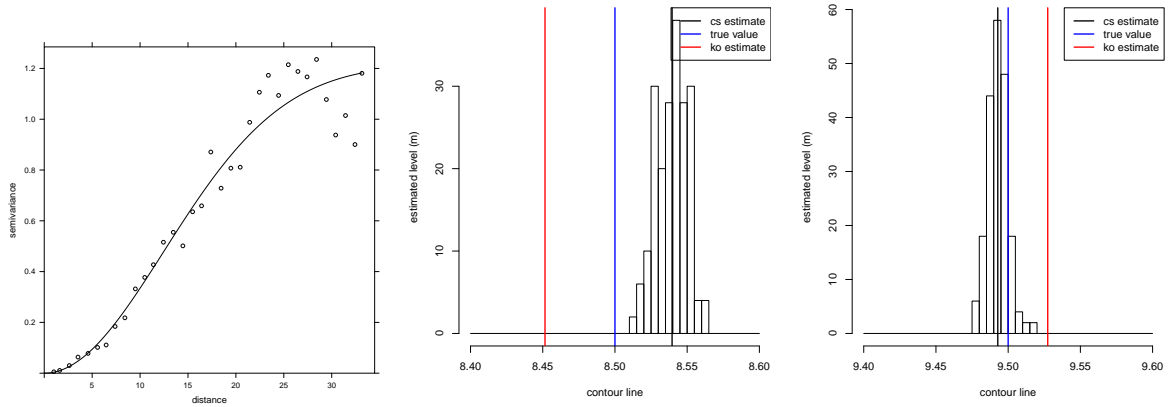


Figure 3: Left: Re-estimated empirical variogram from the $n = 250$ data points; Right: estimated elevation for C_1 and C_2 .

three places. This behaviour can be explained by the fact that very few topographic points are available around this pool.

On the contrary, the field reconstructed with the ordinary kriging method shows greater difference to the true field especially on the top part of the domain, despite a high concentration of ground-truth surveys.

To better assess the precision given by the two approaches, the root mean square difference e between results and true field is computed. The error value obtained without considering the contour polylines is equal to 0.232 m, and to 0.199 m for the proposed method.

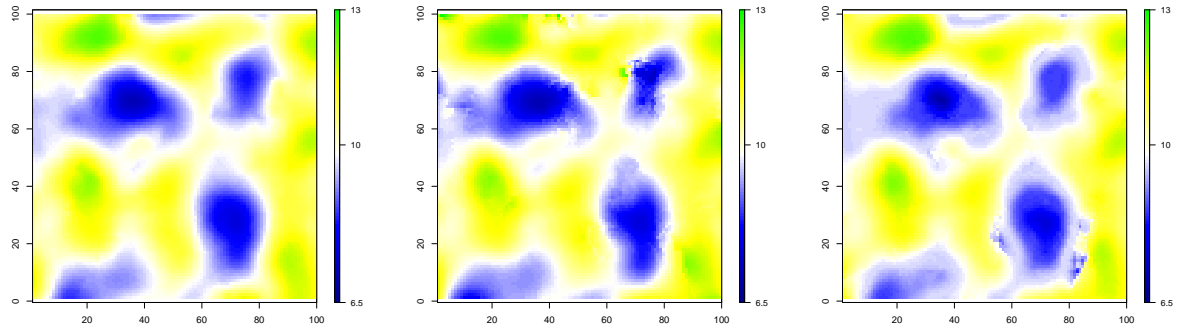


Figure 4: **Reconstructed elevation fields:** Left: true field D ; Middle: ordinary kriging reconstructed field; Right: method (polyline conditional simulation) reconstructed field

This first test suggests that the sampling procedure may influence the results, at least through the location of acquisition points. To check the robustness of the proposed approach, the process described above was repeated 100 times, changing the 250 points data sampling.

Figure 5-left shows the contour polyline C_1 and C_2 error distribution obtained. Figure 5-right shows the mean distance to the true field distribution. Clearly, the proposed method using conditional simulation is more robust with few error variance. The standard deviation of the results obtained with this approach is 0.056 m (resp. 0.037 m) for the contour line 8.5 (resp. 9.5) compared to 0.183 m (resp. 0.1 m) using the ordinary kriging method.

Rank filtering occurred 10% of the times for the C_1 estimation and never for the C_2 estimation. This suggests that rank filtering is useful when contours are in extreme values.

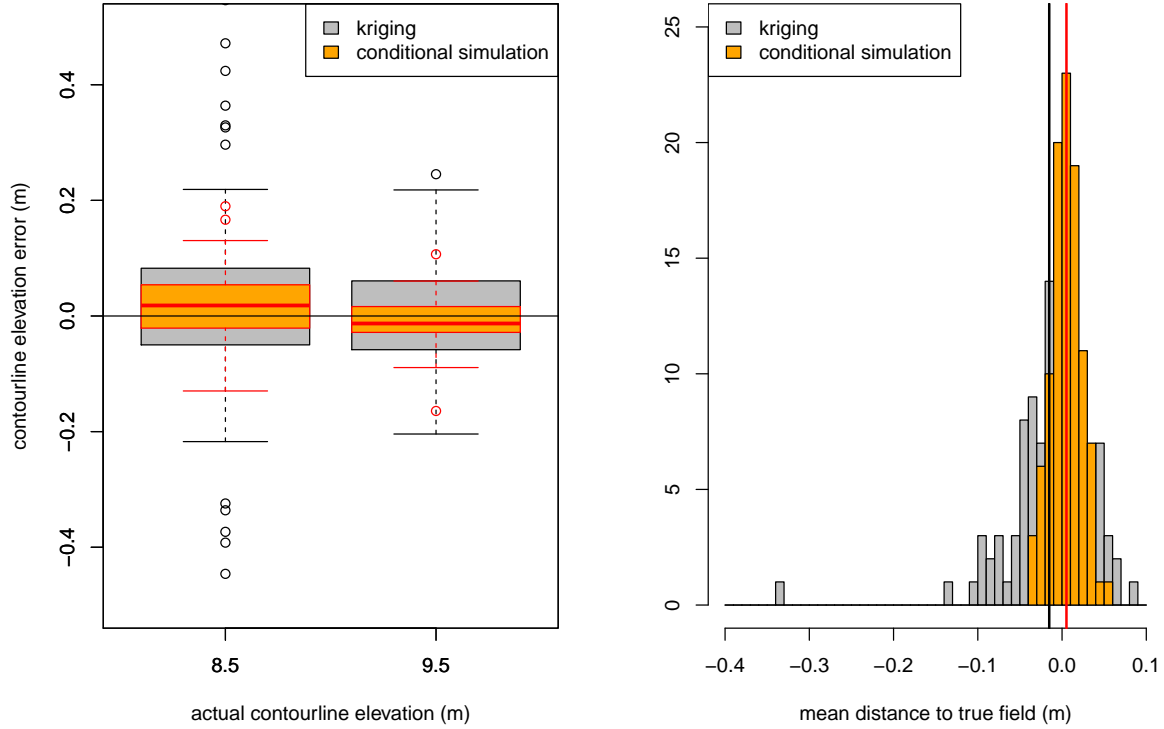


Figure 5: **Errors distribution on 100 random sample sets of 250 data points.** Left: C_j estimation error; Right : mean distance to the true field after reconstruction. The vertical lines represent the mean of the distribution.

Field survey being very costly, the aim is to reduce to the minimum the required elevation data points. The test is thus performed again with different numbers of points. An example of result obtained with a random sample of $N = 50$ points is given in Figure 6. It can be seen that the use of contour line enables to retrieve the pools shapes with better accuracy than an ordinary kriging based only on data points.

The comparison between true field and computed elevation fields with the two approaches is done using the root mean square error. These results are summarized in Table 1 for random samples obtained with $N = 10$ to $N = 250$. As expected, the error decreases if the number of available data points is high and the proposed approach always gives better results than the ordinary kriging.

	$N = 10$	$N = 50$	$N = 100$	$N = 150$	$N = 200$	$N = 250$
e_{ko}	1.064	0.635	0.361	0.403	0.435	0.232
e_{cs}	0.639	0.469	0.329	0.227	0.189	0.199

Table 1: Root mean square errors between true field and reconstructed elevation fields for different N .

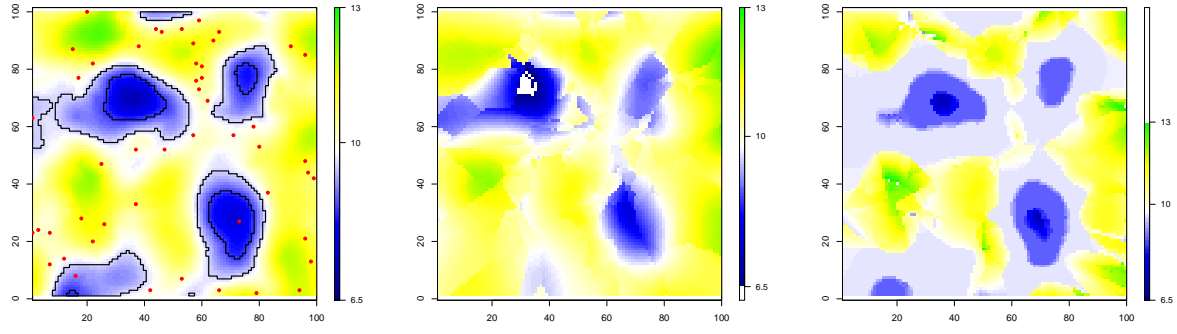


Figure 6: **Reconstructed elevation fields using only 50 data points:** Left: true field D ; Middle: ordinary kriging reconstructed field; Right: method (polyline conditional simulation) reconstructed field.

IV DISCUSSION AND CONCLUSION

The objective of this work was to put forward a methodology to enhance the accuracy of the topographic description required by numerical hydrodynamic modelling, by using information of level lines available from remote-sensing data.

The first results obtained on a totally theoretical example, show that the topographic estimation benefits from such additional data; and the repetition of the process indicates that this result is robust to sampling. If the gain in accuracy may seem limited at this stage (about 3 cm in mean for 250 points), the influence of the sampling rate should be assessed more precisely on the two approaches, since the benefit taken from additional sources of information is expected to increase as less ground-truth data are available.

Moreover, a classical random sampling is obviously not the best approach to conduct a field survey. In the first presented test case, random sampling excluding the direct neighbourhood of the contour lines yielded a lack of data near the pool located at bottom-right part of the domain. This produced irrelevant estimation of the topography in some areas. Further tests are thus planned to infer guidelines in the sampling definition in order to decrease the number of data points required while maintaining a high accuracy in the results, thus enhancing the cost/benefit ratio. In the framework of hydrodynamic modelling, this work will integrate results of uncertainty and sensitivity analyses such as given in Guinot and Cappelaere (2009) or Delenne et al. (2012).

The methodology developed on theoretical test cases, will be assessed in a real-case study of the hydrodynamic modelling of the Vaccares lagoon for which amount of data are available for validation.

References

- Cressie N., Johannesson G. (2008). Fixed rank kriging for very large spatial data sets. *Journal of the Royal Statistical Society: Series B (Statistical Methodology)* 70(1), 209–226.
- Delenne C., Cappelaere B., Guinot V. (2012). Uncertainty analysis of river flooding and dam failure risks using local sensitivity computations. *Reliability Engineering and System Safety* 107, 171–183.
- Guinot V., Cappelaere B. (2009). Sensitivity equations for the one-dimensional shallow water equations: Practical application to model calibration. *Journal of Hydrologic Engineering* 14, 858–861.
- Hostache R., Lai X., Monnier J., Puech C. (2010). Assimilation of spatially distributed water levels into a shallow-water flood model. part ii: Use of a remote sensing image of mosel river. *Journal of Hydrology* 390(3-4), 257 – 268.

- Lindgren G., Rychlik I. (1995). How reliable are contour curves? confidence sets for level contours. *Bernoulli*, 301–319.
- Ogilvie A., Belaud G., Delenne C., Bader J.-C., Oleksiak A., Bailly J. S., Ferry L., Martin D. (2015). Decadal monitoring of the Niger Inner Delta flood dynamics using MODIS optical data. *Journal of Hydrology* 523, 358–383.
- Saito H., Goovaerts P. (2000). Geostatistical interpolation of positively skewed and censored data in dioxin-contaminated site. *Environmental Science Technology* 34, 4228–4235.
- Schumann G., Matgen P., Hoffmann L., Hostache R., Pappenberger F., Pfister L. (2007). Deriving distributed roughness values from satellite radar data for flood inundation modelling. *Journal of Hydrology* 344(1-2), 96 – 111.
- Wameling A., Saborowski J. (2001). Construction of local confidence intervals for contour lines. In *Proceedings of the IUFR4.11 Conference in forest biometry*.
- Yamamoto J. K. (2000). An alternative measure of the reliability of ordinary kriging estimates. *Mathematical Geology* 32, 489–509.
- Yamamoto J. K. (2007). On unbiased back-transform of lognormal kriging estimates. *Computacional Geosciences* 11, 219–234.